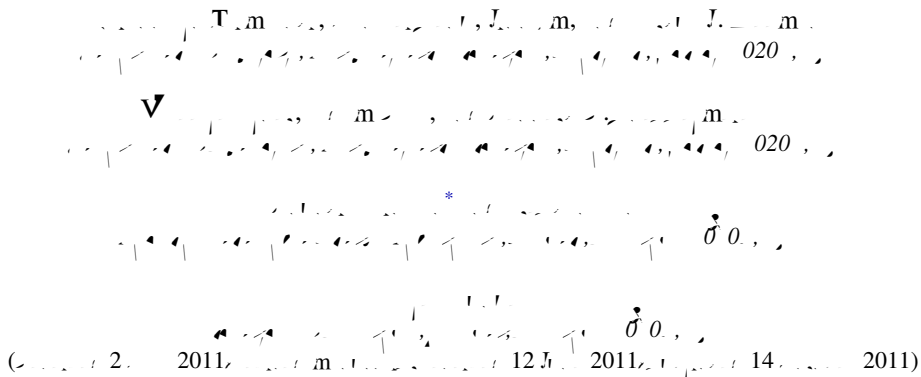


## Using design principles to systematically plan the synthesis of hole-conducting transparent oxides: Cu<sub>3</sub>VO<sub>4</sub> and Ag<sub>3</sub>VO<sub>4</sub> as a case study



The crystal structure of Cu<sub>3</sub>VO<sub>4</sub> (top) and Ag<sub>3</sub>VO<sub>4</sub> (middle) is based on the data from [2, 2011] and [12, 14, 2011]. The structure is based on the data from [2, 2011] and [12, 14, 2011]. The structure is based on the data from [2, 2011] and [12, 14, 2011]. The structure is based on the data from [2, 2011] and [12, 14, 2011].

The crystal structure of Cu<sub>3</sub>VO<sub>4</sub> (top) and Ag<sub>3</sub>VO<sub>4</sub> (middle) is based on the data from [2, 2011] and [12, 14, 2011]. The structure is based on the data from [2, 2011] and [12, 14, 2011]. The structure is based on the data from [2, 2011] and [12, 14, 2011]. The structure is based on the data from [2, 2011] and [12, 14, 2011].

### I. DESIGN PRINCIPLES OF p-TYPE TRANSPARENT CONDUCTING OXIDES

The design principles for p-type transparent conducting oxides (TCOs) are based on the following criteria: (1) high optical transparency in the visible range, (2) high electrical conductivity, (3) low carrier concentration, and (4) high carrier mobility. The design principles for p-type TCOs are based on the following criteria: (1) high optical transparency in the visible range, (2) high electrical conductivity, (3) low carrier concentration, and (4) high carrier mobility.





... **m** ... **f** ... **m** ... **f** ...  
... **m** ...

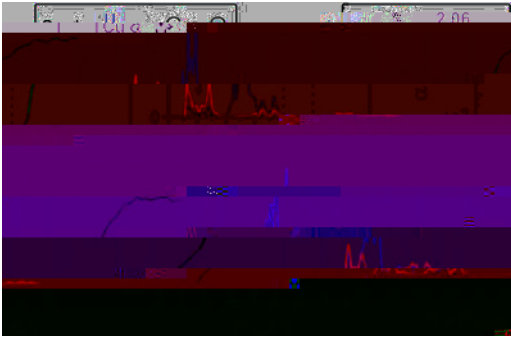


Fig. 4. (Color online) Energy band structure of  $\text{Cu}_2\text{O}$  and  $\text{Ag}_2\text{O}$  (see text for details). The conduction bands (C1, C2, C3) and valence bands (V1, V2, V3) are shown. The band gap is indicated by the dashed line. The energy scale is in eV and the momentum scale is in  $\text{Å}^{-1}$ .

**C. Band-structure properties of  $\text{Cu}_2\text{O}$  and  $\text{Ag}_2\text{O}$ : Optical properties of the binaries**

Figure 4 shows the energy band structure of  $\text{Cu}_2\text{O}$  and  $\text{Ag}_2\text{O}$ . The conduction bands (C1, C2, C3) and valence bands (V1, V2, V3) are shown. The band gap is indicated by the dashed line. The energy scale is in eV and the momentum scale is in  $\text{Å}^{-1}$ .





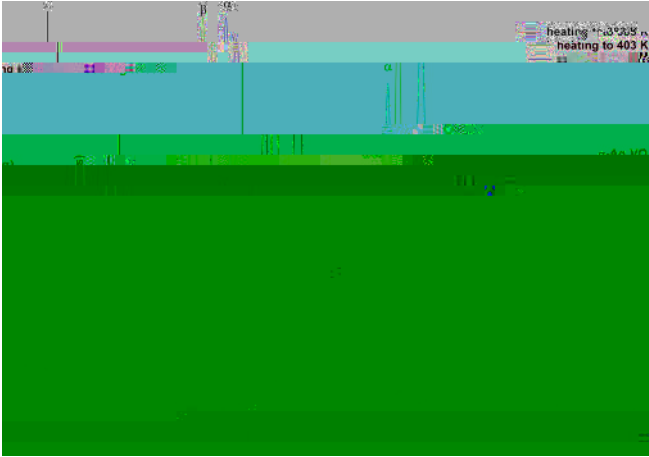


Fig. 1. XRD patterns of  $\text{Cu}_3\text{VO}_4$  (blue) and  $\text{Ag}_3\text{VO}_4$  (green) prepared by the sol-gel method. The inset shows the enlarged view of the peak at  $2\theta \approx 21.5^\circ$ .

The XRD patterns of  $\text{Cu}_3\text{VO}_4$  and  $\text{Ag}_3\text{VO}_4$  prepared by the sol-gel method are shown in Fig. 1. The patterns show a sharp peak at  $2\theta \approx 21.5^\circ$  for  $\text{Cu}_3\text{VO}_4$  and a broader peak at the same position for  $\text{Ag}_3\text{VO}_4$ . The inset shows the enlarged view of the peak at  $2\theta \approx 21.5^\circ$ . The peak at  $2\theta \approx 21.5^\circ$  is assigned to the (110) plane of  $\text{Cu}_3\text{VO}_4$  and  $\text{Ag}_3\text{VO}_4$ . The intensity of the peak at  $2\theta \approx 21.5^\circ$  is higher for  $\text{Cu}_3\text{VO}_4$  than for  $\text{Ag}_3\text{VO}_4$ . This indicates that  $\text{Cu}_3\text{VO}_4$  has a higher degree of crystallinity than  $\text{Ag}_3\text{VO}_4$ . The XRD patterns of  $\text{Cu}_3\text{VO}_4$  and  $\text{Ag}_3\text{VO}_4$  are indexed to the  $\text{Cu}_3\text{VO}_4$  and  $\text{Ag}_3\text{VO}_4$  phases, respectively. The XRD patterns of  $\text{Cu}_3\text{VO}_4$  and  $\text{Ag}_3\text{VO}_4$  are shown in Fig. 1. The patterns show a sharp peak at  $2\theta \approx 21.5^\circ$  for  $\text{Cu}_3\text{VO}_4$  and a broader peak at the same position for  $\text{Ag}_3\text{VO}_4$ . The inset shows the enlarged view of the peak at  $2\theta \approx 21.5^\circ$ . The peak at  $2\theta \approx 21.5^\circ$  is assigned to the (110) plane of  $\text{Cu}_3\text{VO}_4$  and  $\text{Ag}_3\text{VO}_4$ . The intensity of the peak at  $2\theta \approx 21.5^\circ$  is higher for  $\text{Cu}_3\text{VO}_4$  than for  $\text{Ag}_3\text{VO}_4$ . This indicates that  $\text{Cu}_3\text{VO}_4$  has a higher degree of crystallinity than  $\text{Ag}_3\text{VO}_4$ . The XRD patterns of  $\text{Cu}_3\text{VO}_4$  and  $\text{Ag}_3\text{VO}_4$  are indexed to the  $\text{Cu}_3\text{VO}_4$  and  $\text{Ag}_3\text{VO}_4$  phases, respectively.

**B. Intrinsic defects, hole generation, and hole density in  $\text{Cu}_3\text{VO}_4$  and  $\text{Ag}_3\text{VO}_4$**

$$n(T) = n_0 \exp\left(-\frac{E_a}{kT}\right) \quad (1)$$





m f  
 f m m f m m  
 m f ff ( ) f m  
 m m 32,33 \*

(

...  $f$  ...  $m$  ...  $f$  ...  
 $4 \parallel m$  ...  $m$  ...  $f$  ...  
 $m$  ...  $0$  ...  $m$  ...  
 $m$  ...  $f$  ...  
 $\mathbf{V}_{3 \times 4}$  ...  $f$  ...  
 $m$  ...  $f$  ...  $\mathbf{V}_{3 \times 4}$  ...  $\mathbf{V}_{3 \times 4}$  ...  
 $\mathbf{T}$  ...  $\mathbf{V}_{3 \times 4}$  ...  
 $m$  ...  $f$  ...  $\mathbf{T}$  ...  
 $m$  ...  $f$  ...  $\mathbf{V}_{3 \times 4}$  ...  
 $\mathbf{T}$  ...  $f$  ...  $\mathbf{V}_{3 \times 4}$  ...





